

# Forecast on the Productivity of a Multiple Effects Plan Solar Distiller

Dobet Dago Djaman Ives N'drin, Siaka Touré, Adingra Paul Arsène Kouassi 

Laboratory of Matter, Environmental and Solar Energy Sciences (LASMES), UFR Sciences of the Structures of the Material and Technology, Félix Houphouët Boigny University, Abidjan, Côte d'Ivoire

Email: ivesisrael15@gmail.com, siakaahtoure@yahoo.fr, debouegla@yahoo.fr

**How to cite this paper:** N'drin, D.D.D.I., Touré, S. and Kouassi, A.P.A. (2025) Forecast on the Productivity of a Multiple Effects Plan Solar Distiller. *Open Journal of Applied Sciences*, 15, 2149-2175.  
<https://doi.org/10.4236/ojapps.2025.157142>

**Received:** June 16, 2025

**Accepted:** July 21, 2025

**Published:** July 24, 2025

Copyright © 2025 by author(s) and Scientific Research Publishing Inc.  
This work is licensed under the Creative Commons Attribution International License (CC BY 4.0).

<http://creativecommons.org/licenses/by/4.0/>



Open Access

## Abstract

In this study, we first present the operation of a five-compartment solar distiller involving several effects: heat conduction from the absorber of the central compartment (using the principle of hot-box solar stoves) to the tanks of the two compartments containing the water to be distilled and exposed to the sun (using the principle of flat solar distillers with a simple greenhouse effect), and a portion of each of the vapors produced in these two compartments will be diverted to two other compartments for condensation. Secondly, we will predict, for years between 2013 and 2022, the productivity of this distiller as a function of daily irradiation, longitude of location, latitude of location, time zone offset of the location, date of day, start time and end time of the distiller's exposure to the sun.

## Keywords

Solar Distillation, Solar Distiller, Predict, Productivity, Daily Irradiation, Longitude, Latitude, Time Zone Offset, Date, Start Time, End Time

## 1. Introduction

With the world's population soaring, drinking water is becoming scarce. Despite the abundance of water on the planet, 97.2% of this water forms the oceans and seas, which have too high a salt concentration, so a large proportion of the water on the planet is undrinkable and cannot be used to irrigate crops [1].

The supply and management of water for human consumption, agriculture and industry have become yet another problem for governments.

Several processes, such as water desalination, are used to solve this problem.

However, these processes generally consume sickle cell energy, which still poses problems of financing, resource depletion and environmental impact.

This is why solar distillation is a solution, and not the least, to the dual problem of energy and water, since it uses solar energy, which is a clean and renewable source for distillation, to obtain water of acceptable quality.

This study focuses on a multiple effects solar distiller which is a solar distiller with five compartments: a central compartment and four side compartments. It aims to predict the productivity of this solar distiller as a function of daily irradiation, the longitude and latitude of the location, the date of the day, the start and end times of the distiller's exposure to the sun.

## 2. Materials and Research Methods

### 2.1. Presentation of the Distiller

Figure 1 on the following page shows a spatial representation of the solar distiller to be studied and the different "views" (directions and orientations of observation) through which the distillation sections are observed.

Figure 2(a), Figure 3(a) and Figure 3(b) show respectively: the diagram of the "view" of a distiller cross-section in a horizontal plane, the diagram of "view 1" in the plane of symmetry plane along axis 1 ↔ 2 (or axis North-South) and the diagram of "view 4" in the plane of symmetry along axis 3 ↔ 4 (or axis East-West) of the distiller (Figure 1).

The distiller we are describing is a solar distiller with two vertical planes of symmetry. The intersection of the first plane of symmetry with a absorbeur's horizontal plane forms the axis marked "1 ↔ 2" (or axis North-South) and the intersection of the second plane with this horizontal plane forms the axis marked

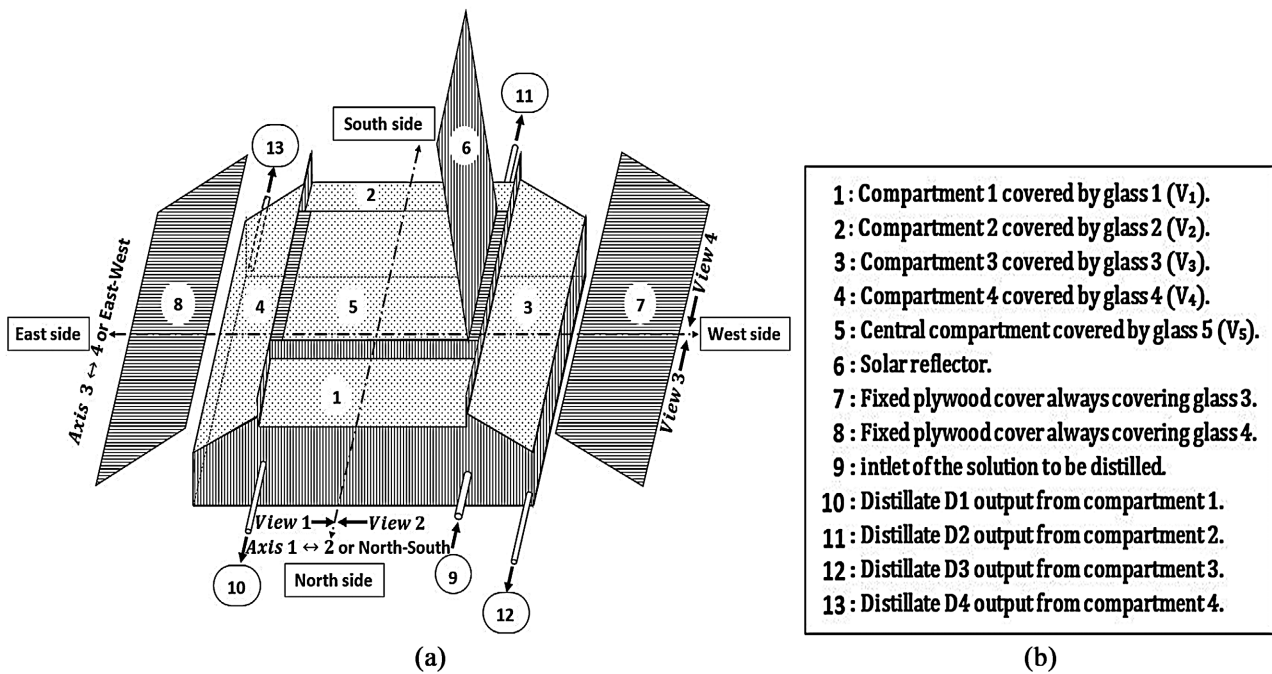
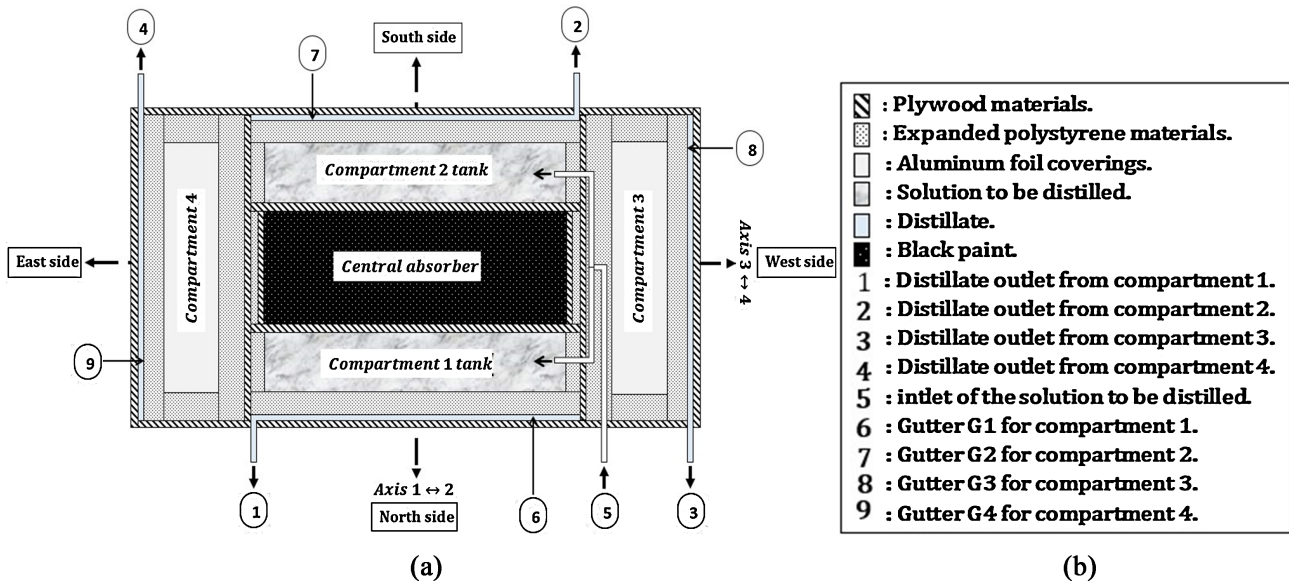
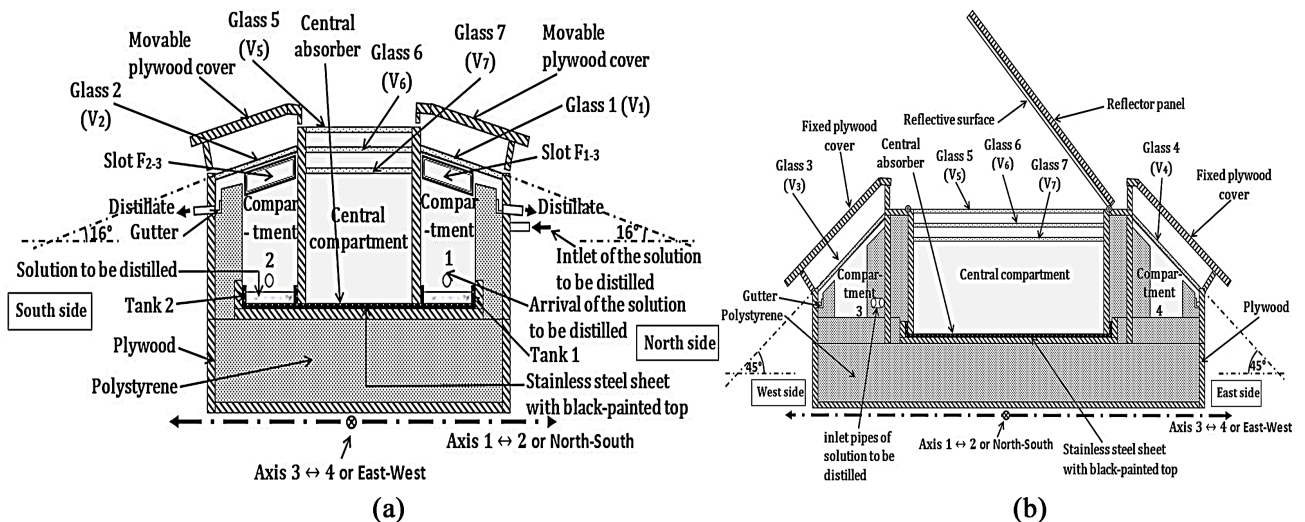


Figure 1. Three-dimensional view of the solar distiller (the dimensions on the drawing are not proportional to the actual dimensions). (a) Three-dimensional view; (b) Legend of figure.



**Figure 2.** Top view of a horizontal section of the solar distiller (Dimensions on the drawing are not proportional to the actual dimensions). (a) Top view; (b) Legend of the figure.



**Figure 3.** View 1 of section along axis 1 ↔ 2 and view 4 of section along axis 3 ↔ 4. (Dimensions on the drawing are not proportional to the actual dimensions). (a) View 1; (b) View 4.

“3 ↔ 4” (or axis East-West) (Figures 1-3).

The distiller has five compartments (Figure 1 and Figure 2): the central compartment covered by three glass panes  $V_5$ ,  $V_6$  and  $V_7$ , topped by the vertical reflector panel facing away from the sun and reflecting the sun’s rays above the distiller towards the entrance to the central compartment, at the bottom of which is the central absorber; compartments 1 and 2, covered respectively by glass panes  $V_1$  and  $V_2$ , which can each be covered by one removable plywood cover; at the bottom of compartments 1 and 2 are tanks 1 and 2 respectively, which can contain the solution to be distilled; compartments 3 and 4, each communicating with compartments 1 and 2 via slots  $F_{1-3}$  and  $F_{1-4}$ ,  $F_{2-3}$  and  $F_{2-4}$ , these compartments are

covered respectively by glass panes  $V_3$  and  $V_4$ , each of which is covered by one fixed plywood cover.

It should be noted that the absorber block “tank 1 + absorber + tank 2” is made from the same stainless steel sheet, which is painted with a matt black paint on top.

## 2.2. Elements of the Distiller

### 2.2.1. Glazing

All the distiller's compartments are covered by ordinary glass, all the same thickness of 5 mm.

The thickness of the glass is not too small so that it is more resistant (glass does not break under its own weight or during handling), and not too large so that, when exposed to the sun, it absorbs less solar radiation.

These glass panes have two important features:

- good transmission of visible radiation and opacity to long-wave infrared rays, which promotes both the transmission of solar heat radiation and the greenhouse effect;
- good wettability, which helps condensed water droplets to run off under glass.

Depending on requirements, the glass is used to transmit solar radiation or to condense water vapour.

#### 1) Glass $V_1$ and glass $V_2$

Glass 1 ( $v_1$ ) and glass 2 ( $v_2$ ) cover Compartment 1 and Compartment 2 respectively.

In principle, they play two roles at the same time: transmitting solar radiation, thereby promoting the greenhouse effect, and acting as a condensation surface for the steam produced.

However, they can also be covered by a plywood lid.

In this case, they act as a condensation surface for the water vapour produced.

These two glass panes have the same dimensions:

length: 153 cm

width: 29 cm

thickness: 5 mm

#### 2) Glass $V_3$ and glass $V_4$

Glass 3 ( $v_3$ ) and glass 4 ( $v_4$ ) cover compartment 3 and compartment 4 respectively, each one is covered by a plywood lid.

They act as a condensation surface for the part of the steam produced in compartments 1 and 2 which is diverted through the four slots in compartments 1 and 2 to compartments 3 and 4.

These two glass panes have the same dimensions:

length: 105 cm

width: 34.5 cm

thickness: 5 mm

#### 3) Glass $V_5$ , $V_6$ and glass $V_7$

Glass 5 ( $v_5$ ), Glass 6 ( $v_6$ ) and Glass 7 ( $v_7$ ) cover the central absorber compartment

respectively from top to bottom.

Their role is to transmit solar radiation to the central absorber and promote the greenhouse effect in this compartment.

These two glass panes have the same dimensions:

length: 144.5 cm

width: 44 cm

thickness: 5 mm

### 2.2.2. Central Absorber and Tanks

The central absorber and the two tanks are made from the same 2 mm thick stainless steel sheet, the top surface of which is painted matt black.

#### 1) Central absorber

The central absorber is an empty, parallelepiped-shaped container, the inside surface of which is painted matt black to maximize absorption of solar radiation transmitted through the glass panes of this compartment.

Its dimensions are (Figure 4):

length: 149.5 cm

width: 44 cm

hauteur: 4 cm

For this distiller, the ratio between the width  $l$  and length  $L$  of the central absorber is:

$$l/L = 0.3045$$

#### 2) Tanks

Tank 1 and Tank 2 are parallelepiped-shaped container whose inner surfaces

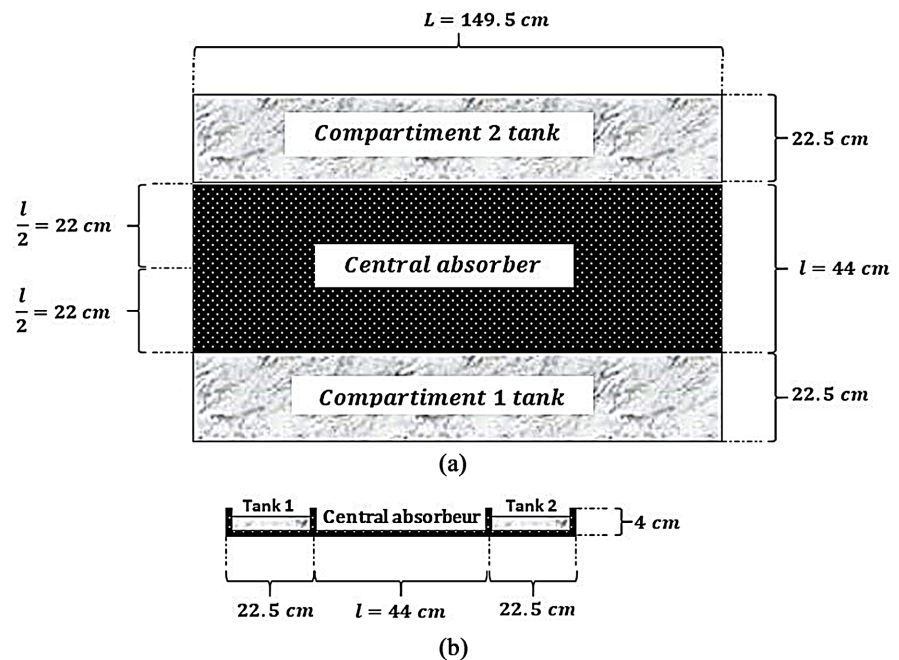


**Figure 4.** Dimensions of the block “Tank 1 + Central absorber + Tank 2”. (a) Top view; (b) Profile view.

are painted matt black to optimize absorption of solar radiation.

These two tanks receive the solution to be distilled and heat it for evaporation.

These two trays are located at the base of Compartment 1 and Compartment 2 respectively, and are attached to the central absorber.

These two bins have the same dimensions, which are (Figure 4):

length: 149.5 cm

width: 22.5 cm

thickness: 4 cm

### 2.2.3. Reflector Panel

The reflector panel is made of rectangular plywood and has one side covered with reflective plastic sheeting.

This panel has two roles depending on experimental requirements:

- when the contribution of the central compartment is required for heating, it is in a vertical position, against the sun, to reflect part of the solar rays passing over the distiller towards the entrance to the central compartment;
- when the contribution of the central compartment to heating is not required, it is in the horizontal position to cover the upper glass pane ( $V_5$ ) of the central compartment to prevent sunlight from entering the central compartment.

Its dimensions are:

length: 145 cm

width: 45 cm

thickness: 1.5 cm

### 2.2.4. Plywood Covers

Plywood lids cover the windows to prevent solar radiation from reaching them (to prevent solar radiation from passing through them or heating them up by absorbing part of this radiation).

They allow natural air circulation between the lids and the glass panes they cover (natural convection cooling glass panes)

This can lead to condensation of water vapour under the inner surface of the glass panes.

#### 1) Cover 1 and cover 2

The cover 1 and cover 2 are rectangular, movable and may or may not cover glass panes

$V_1$  and  $V_2$  respectively, as required. These covers have the same dimensions:

length: 163 cm

width: 39 cm

thickness: 1.5 cm

#### 2) Cover 3 and cover 4

The cover 3 and cover 4 are rectangular, fixed and always cover glass panes  $V_3$  and  $V_4$  respectively.

These covers have the same dimensions:

length: 115 cm

width: 35.5 cm  
thickness: 1.5 cm

### 2.2.5. Thermal Insulation

Thermal insulation minimizes heat loss by thermal conduction to the outside of the distiller.

For the distiller, the thermal insulators used are:  
plywood and expanded polystyrene.

The arrangement and dimensions of these two insulators depend on the position of the distiller's outer walls:

- to minimize losses through the four external side walls (vertical walls), we use the same layout (from inside to outside): a 7.5 cm thick block of polystyrene, followed by 1.5 cm thick plywood, as shown in **Figure 5**.

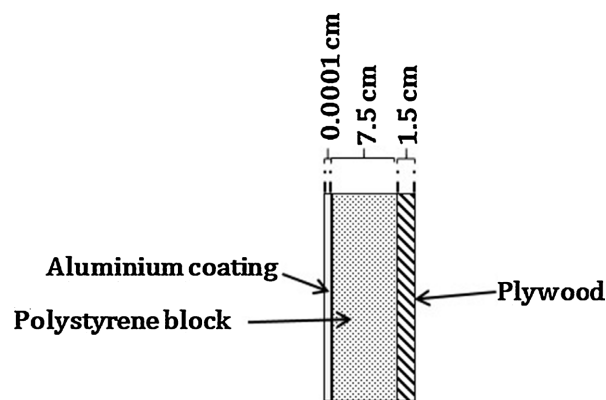


**Figure 5.** Thermal insulation arrangement for a distiller side wall.

- for downward heat loss, the insulation consists of 1.5 cm thick plywood, which supports the “tray 1 + central absorber + tray 2” block, a 15 cm thick block of polystyrene and then 1.5 cm thick plywood, as shown in **Figure 6**.

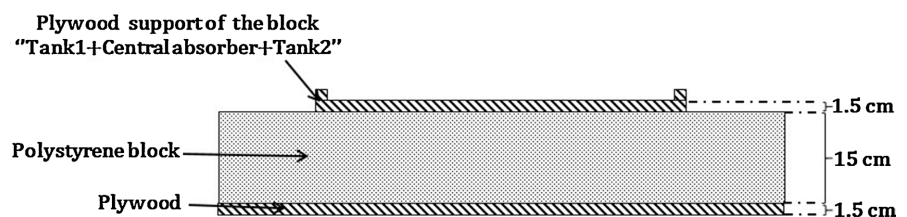


**Figure 6.** Thermal insulation arrangement for the distiller base.

## 2.3. Principle of the Solar Distiller

The central absorber is heated by solar radiation transmitted through the glass panes, it is accentuated by the greenhouse effect.

Since the central absorber and the two tanks are made from the same stainless steel sheet, heat is transferred from the central absorber to the two tanks by conduction within the sheet.

In addition to the heat transferred by conduction to the tanks, heat is also

transferred by solar radiation transmitted through each pane of glass in compartments 1 and 2, to the solution to be distilled and to tanks 1 and 2 (Figure 7).

As a result, water evaporates from the solution to be distilled in tanks 1 and 2, whose vapors rise by natural convection respectively, towards glass panes  $V_1$  and  $V_2$  respectively.

Some of the vapors from compartments 1 and 2 condense under the glass panes  $V_1$  and  $V_2$  into droplets which are collected by the respective gutters of compartments 1 and 2 to form, at their outlets, the distillates (also known as condensates) from compartments 1 and 2.

The other part of the steam from compartment 1 is diverted through slots  $F_{1-3}$  and  $F_{1-4}$  to compartments 3 and 4, and the other part of the steam from compartment 2 is diverted through slots  $F_{2-3}$  and  $F_{2-4}$  into compartments 3 and 4.

These vapors from compartments 1 and 2 into compartments 3 and 4 condense under their respective panes  $V_3$  and  $V_4$  to form distillates from compartments 3 and 4.

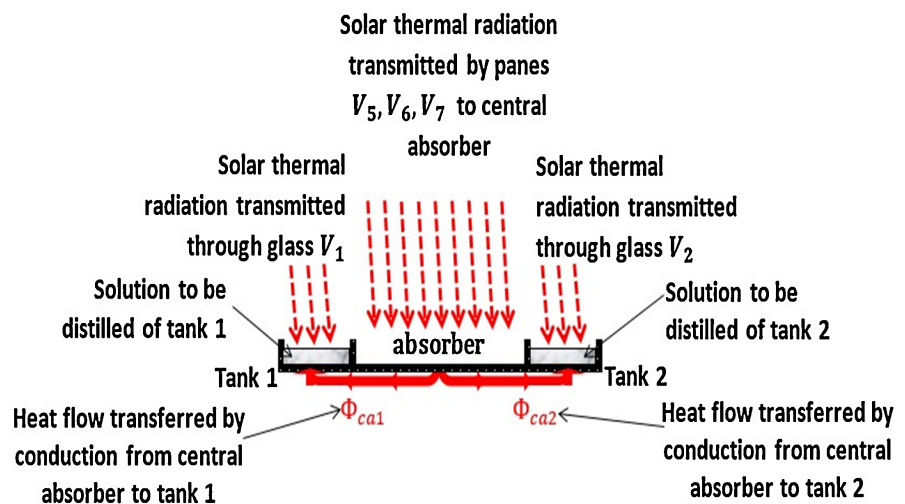


Figure 7. Heat conduction between the central absorber and the two glass panes.

## 2.4. Material

### 2.4.1. Irradiance

Figure 8 show several instruments.

Figure 8(a): the “EPPLEY PsP” pyranometer, used to measure irradiance received on a horizontal surface, with a flat solar sensor inside that can receive solar radiation at a solid angle of  $2\pi$  steradians, the pyranometer delivers a millivolt voltage, proportional to the irradiance received  $E = \frac{V}{k}$  where  $E$  is the irradiance received by the pyranometer in  $W/m^2$ ,  $V$  is the potential difference delivered by the pyranometer in mV and  $k = 10.41 \times 10^{-3} \text{ mV}\cdot\text{m}^2/\text{W}$  is the pyranometer’s proportionality coefficient.

**Figure 8(b):** the “PICO” brand voltage recorder with a U.S.B. cable for connection to a computer.

**Figure 8(c):** the computer to which the voltage recorder is connected.

It should be noted that irradiance is recorded every minute.

**Figure 9(a)** shows the experimental set-up on the roof of the research building.

This **Figure 9(a)** including: solar distiller, pyranometer, thermocouples and recording unit.

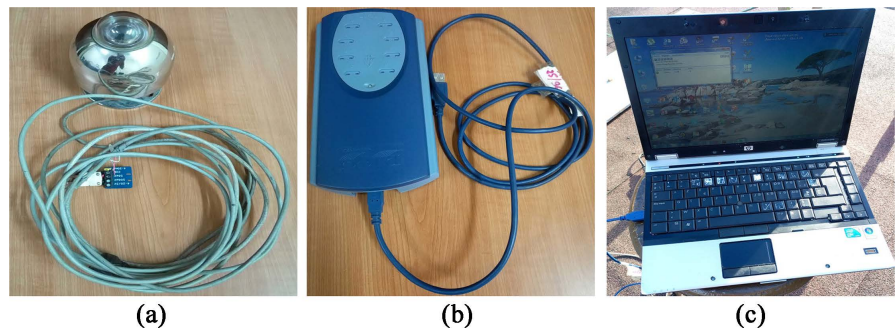


**Figure 8.** Three devices used to record irradiance. (a) Pyranometer; (b) Data logger; (c) Computer.

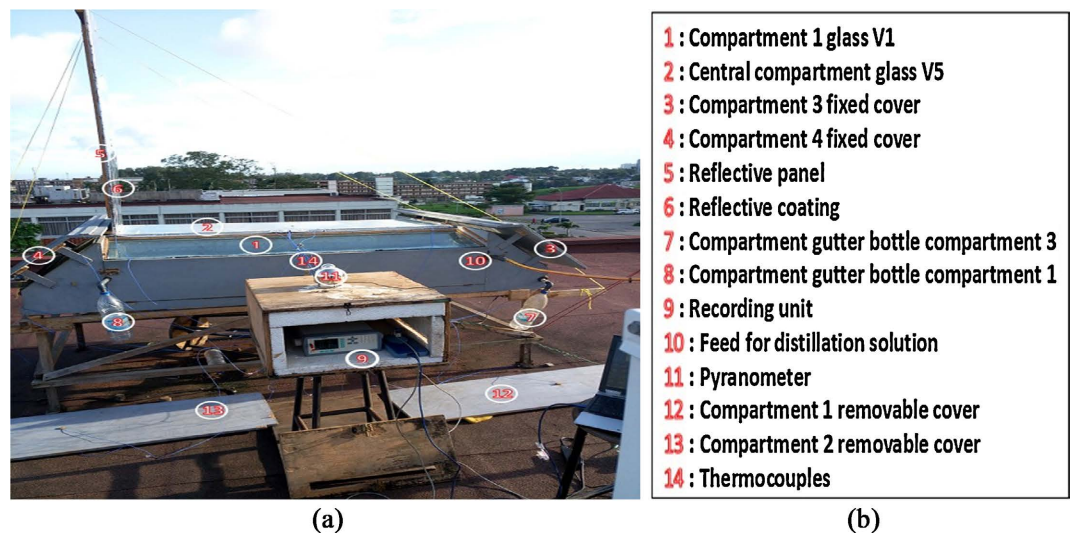


**Figure 9.** The experimental set-up. (a) Distiller, thermocouples, recording unit and pyranome; (b) Legend of the figure ter.

### 2.4.2. Distillate Quantity

**Figure 10** shows the “SF-400C” electronic balance with digital display used to measure the masses (in grams to an accuracy of 0.01 g) of distillates collected 2 hours 30 minutes after the start of the experiments, then every 1 hour until the end of the experiment.

## 2.5. Research Methods

### 2.5.1. Daily Irradiation

The daily solar irradiation  $I$  is the solar energy received per unit area over the

entire duration  $\Delta t = t_f - t_i$  of the day's experiment, from the initial instant  $t_i$  (the 1<sup>st</sup> measurement) to the final instant  $t_f$  (the last measurement) with  $\Delta_t = 10$  h30 min = 10.5 h, it is given by the formula:



**Figure 10.** “SF-400C” electronic scale.

$$I = \int_{t_i}^{t_f} E(t) dt \tag{1}$$

where  $I$  is in Wh/m<sup>2</sup>,  $E(t)$  is irradiance at time  $t$  in W/m<sup>2</sup>.

**2.5.2. Productivity**

Productivity  $P_r$  in kg/m<sup>2</sup> is the total mass of water collected per unit area of the water tanks [2]:

$$P_r = \frac{m_d}{2 \times S_1} \tag{2}$$

where  $m_d$  is the total mass of water collected from compartments 1, 2, 3 and 4 in kg and  $S_1$  is the surface area of one of the tanks in m<sup>2</sup>.

**2.5.3. Declination  $\delta$**

The declination  $\delta$  is given by the formula proposed by Vincent Bourdin:

$$\delta = 0.38 + 23.26 \times \sin\left(\frac{360 \times n_0}{365.24} - 1.395\right) + 0.375 \times \sin\left(\frac{2 \times 360 \times n_0}{365.24} - 1.47\right) \tag{3}$$

where  $n_0$  is the number of the day of the year, counted from January 1, 2013 to December 31, 2023 ( $n_0 = 1$  on January 1, 2013) and  $\delta$  in degrees of arc [3].

**2.5.4. Hour Angle  $W$**

At the location under consideration, we have:

$$H_{slv} = H_{ml} - \frac{E_T}{60}$$

where  $H_{slv}$  is local true solar time,  $H_{ml}$  is local mean solar time and  $E_T$  is the equation of time in minute also proposed by Vincent Bourdin:

$$E_T = 7.36 \times \sin\left(\frac{360 \times n_0}{365.242} - 0.071\right) + 9.92 \times \sin\left(\frac{2 \times 360 \times n_0}{365.42} + 0.357\right) + 0.305 \times \sin\left(\frac{3 \times 360 \times n_0}{365.42} + 0.256\right) \tag{4}$$

where  $n_0$  is the number of the day of the year, counted from January 1, 2013 to December 31, 2023 ( $n_0 = 1$  on January 1, 2013) [3].

We have the following relationships:

$$\begin{cases} H_l = T.U + \Delta H \\ H_{ml} = T.U + \frac{\lambda}{15} \end{cases}$$

where  $H_l$  is local time,  $T.U$  is universal time,  $\Delta H$  is the time zone offset and  $\lambda$  is the longitude of the location.

We can write that with formulas (2.5.4) and (2.5.4):

$$H_{svl} - \frac{E_T}{60} = H_l - \Delta H - \frac{E_T}{60} \quad (5)$$

Since  $H_{svl} = \frac{W}{15} + 12$ , where  $w$  is the hour angle in degrees of arc, we finally find:

$$w = 15 \times H_l + \lambda - 15 \times \Delta H - \frac{E_T}{4} - 180 \quad (6)$$

Instead of experimenting, we have the following data:

Longitude  $\lambda = -3.98833333333^\circ$ , latitude  $L = +5.34472222222^\circ$ , time zone offset  $\Delta H = 0$  hour, so:

$$w = 15 \times H_l - 186.98833333333 - \frac{E_T}{4} \quad (7)$$

### 2.5.5. Locating the Sun's Direction

**Figure 11(a)** and **Figure 11(b)** show the three-dimensional local Cartesian reference frame (O, X, Y, Z) linked to the central compartment with the sun's height  $h$  and azimuth  $a$ , then in two dimensions on the central absorber.

Consider the vectors  $i, j, k$  which are the respective unitary director vectors of these axes. In this reference frame, the coordinates of the vector  $\mathbf{u} \begin{pmatrix} x \\ y \\ z \end{pmatrix}$  which

is the unitary directing vector of the line passing through the origin O of the reference frame, through the center of the sun and towards the sun, are such that:

$$\begin{cases} x = \cos h \times \cos a \\ y = -\cos h \times \sin a \\ z = \sin h \end{cases} \quad (8)$$

or:

$$\begin{cases} x = \cos \delta \times \sin L \times \cos W - \cos L \times \sin \delta \\ y = -\cos \delta \times \sin W \\ z = \cos \delta \times \cos L \times \cos W + \sin L \times \sin \delta \end{cases} \quad (9)$$

**Figure 12(a)** and **Figure 12(b)** show vector  $\mathbf{u}_{xz}$  which is the projection of vector  $\mathbf{u}$  in the (OXZ) plane, and vector  $\mathbf{u}_{yz}$  that of vector  $\mathbf{u}$  in the (OYZ) plane. We define the following angle measures:

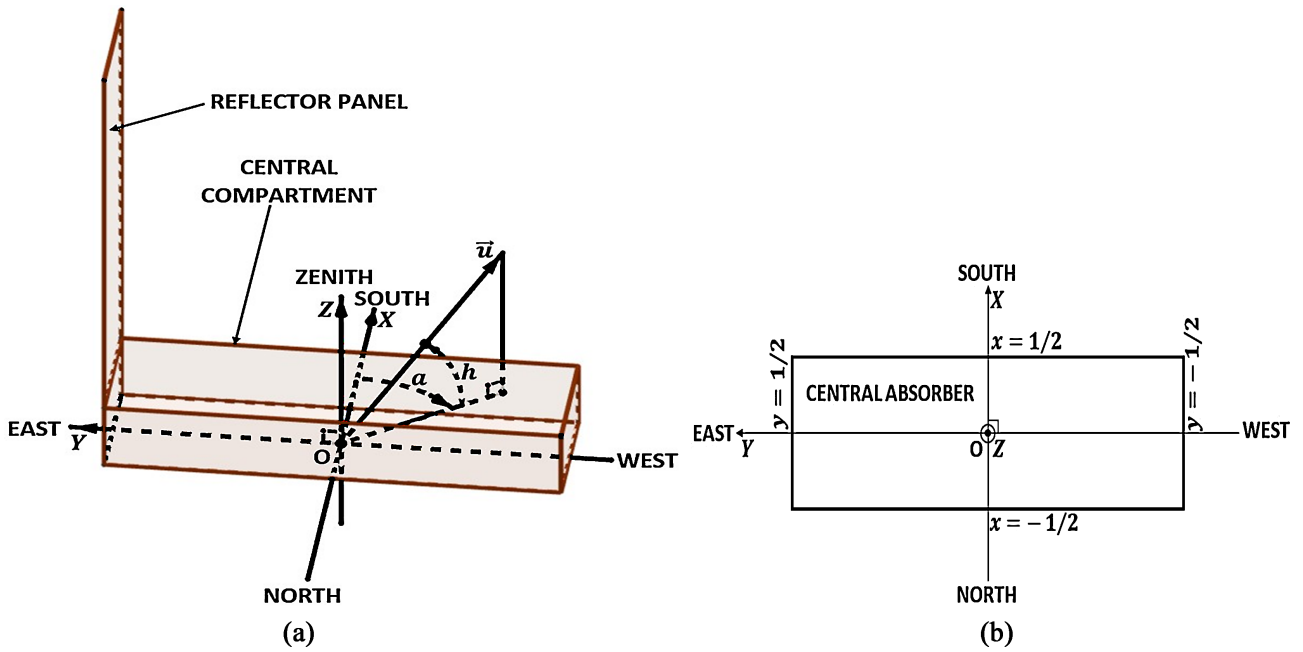


**Figure 11.** Local Cartesian coordinate system linked to the distiller. (a) Local three-dimensional Cartesian coordinate system linked to the distiller (with the sun positioned in the afternoon); (b) Local Cartesian reference frame linked to the distiller (top view).

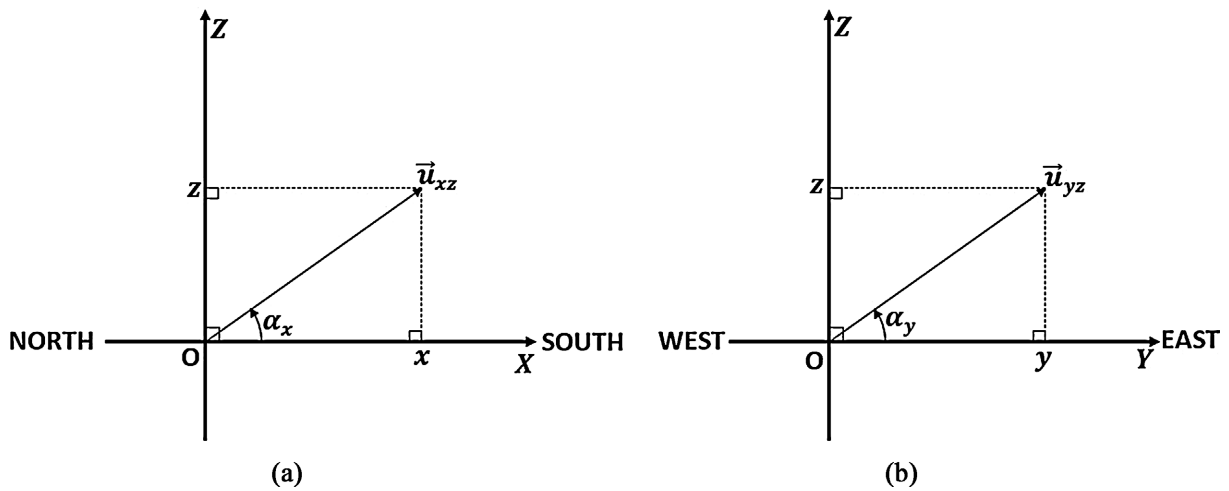


**Figure 12.** Projection of the vector  $u$  in the (OXZ) and (OYZ) planes. (a) Projection of the vector  $u$  in the (OXZ) plane (b) Projection of the vector  $u$  in the (OYZ) plane.

$$\begin{cases} \alpha_x = \text{Mes}(\widehat{i, u_{xz}}) \text{ et } \alpha_x \in [0^\circ; 180^\circ] \\ \alpha_y = \text{Mes}(\widehat{i, u_{yz}}) \text{ et } \alpha_y \in [0^\circ; 180^\circ] \end{cases} \quad (10)$$

In addition

$$\begin{cases} \cos \alpha_x = \frac{x}{\sqrt{x^2 + z^2}} \\ \sin \alpha_x = \frac{z}{\sqrt{x^2 + z^2}} \end{cases} \text{ et } \begin{cases} \cos \alpha_y = \frac{y}{\sqrt{y^2 + z^2}} \\ \sin \alpha_y = \frac{z}{\sqrt{y^2 + z^2}} \end{cases} \quad (11)$$

### 2.5.6. Absolute Mean Angle

The angular deviation between the direction of the sun and the vertical plane passing through the East-West axis is characterized by the angle measure defined by:  $\alpha_{xz} = Mes(\mathbf{u}_{xz}, \hat{\mathbf{k}})$  for  $\alpha_x \geq 0$ , during the day (Figure 10). We have:

- if angles are measured in radians

$$\alpha_{xz} = \frac{\pi}{2} - \alpha_x \tag{12}$$

- if angles are measured in degrees of arc

$$\alpha_{xz} = 90 - \alpha_x \tag{13}$$

We can say that:

- if  $\alpha_{xz} > 0$ , then the sun is on the south side of the east-west axis;
- if  $\alpha_{xz} = 0$ , then the sun is above the East-West axis;
- if  $\alpha_{xz} < 0$ , then the sun is on the north side of the east-west axis.

The Figure 13 shows the angle  $\alpha_{xz} = Mes(\mathbf{u}_{xz}, \hat{\mathbf{k}})$  between the direction of the sun and the vertical plane passing through the East-West axis in the (OXZ) plane.

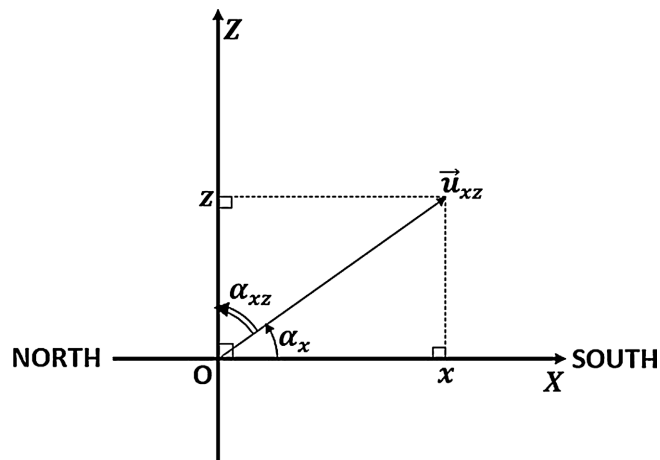


Figure 13. Angle  $\alpha_{xz}$  in the (OXZ) plane.

So, to characterize the proximity of the sun's path (the apparent trajectory of the sun in the sky) to the vertical plane passing through the East-West axis, over the duration of the measurements, we defined the absolute mean angle  $\overline{\alpha_{ax}}$  as the average absolute value of  $\alpha_{xz}$ , relative to the entire measurement time, for values of  $\alpha_x \geq 0$ .

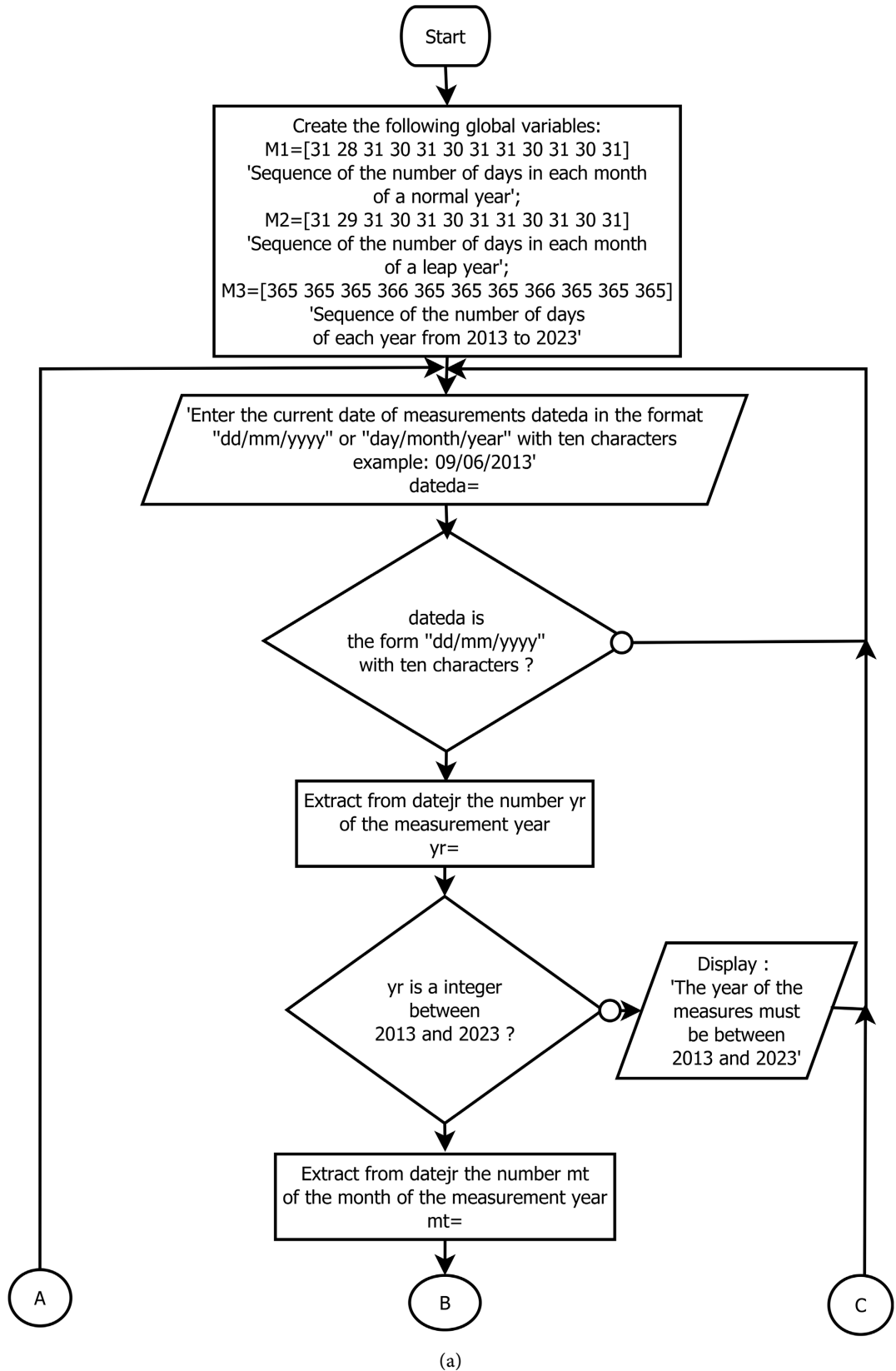
We have:

$$\overline{\alpha_{ax}} = |average(\alpha_{xz})| = \begin{cases} \left| average\left(\frac{\pi}{2} - \alpha_x\right) \right| \\ \text{ou} \\ \left| average(90 - \alpha_x) \right| \end{cases} \tag{14}$$

### 2.5.7. Flowchart for the Absolute Mean Angle $\overline{\alpha_{ax}}$ Calculation

The program for calculating the absolute mean angle  $\overline{\alpha_{ax}}$  is based on the

algorithmic flowchart shown respectively in **Figures 14-17**.



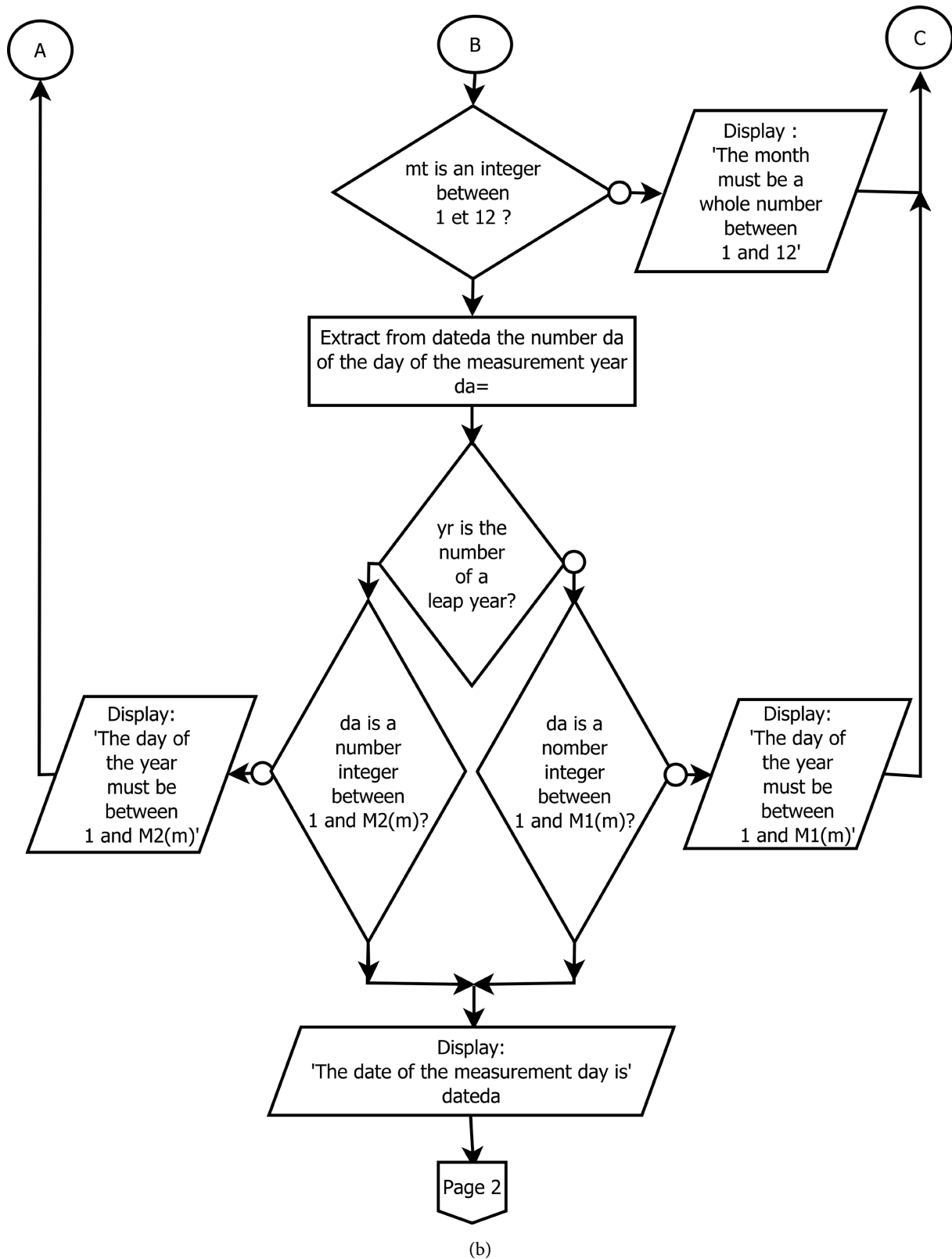
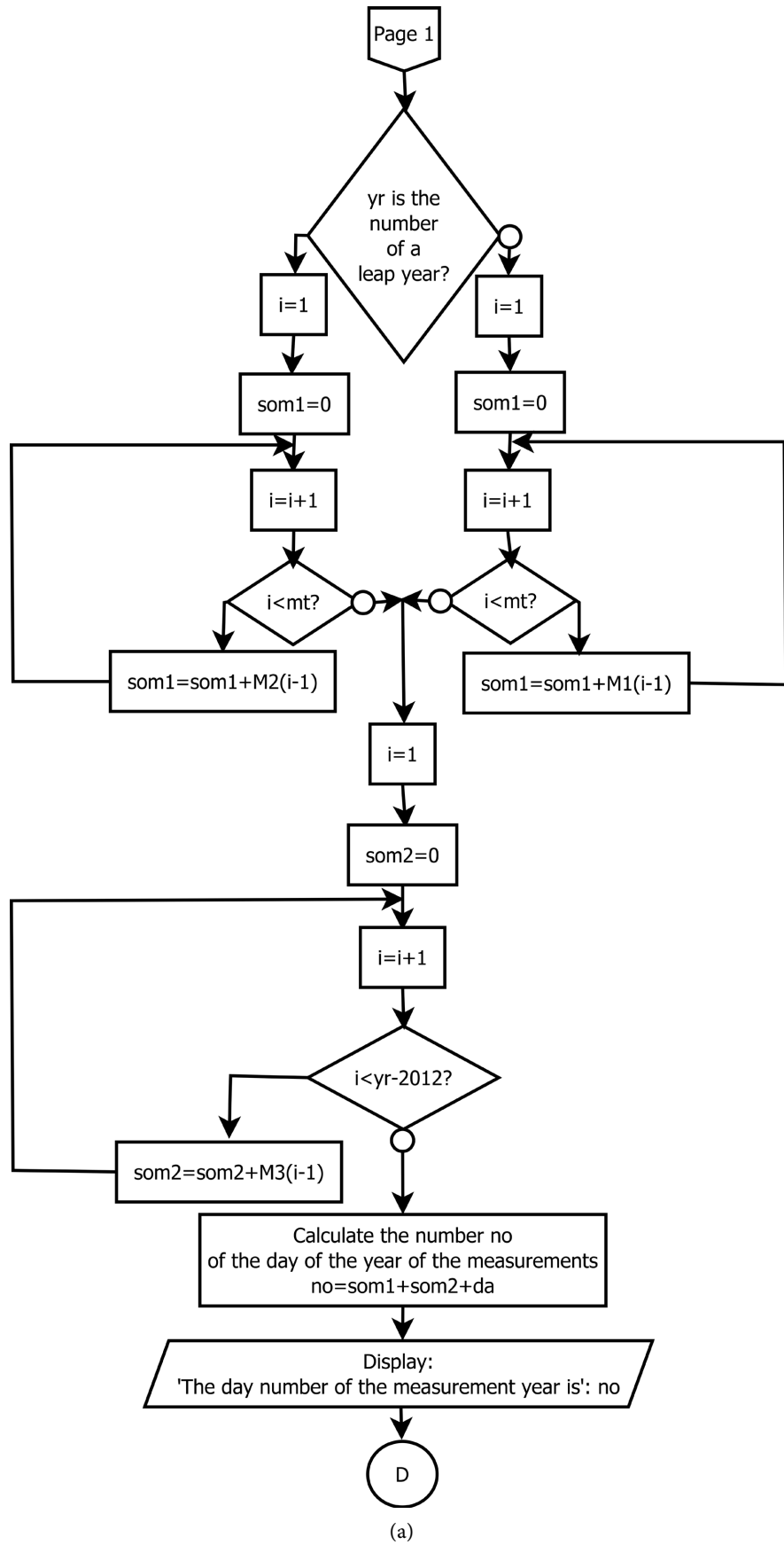
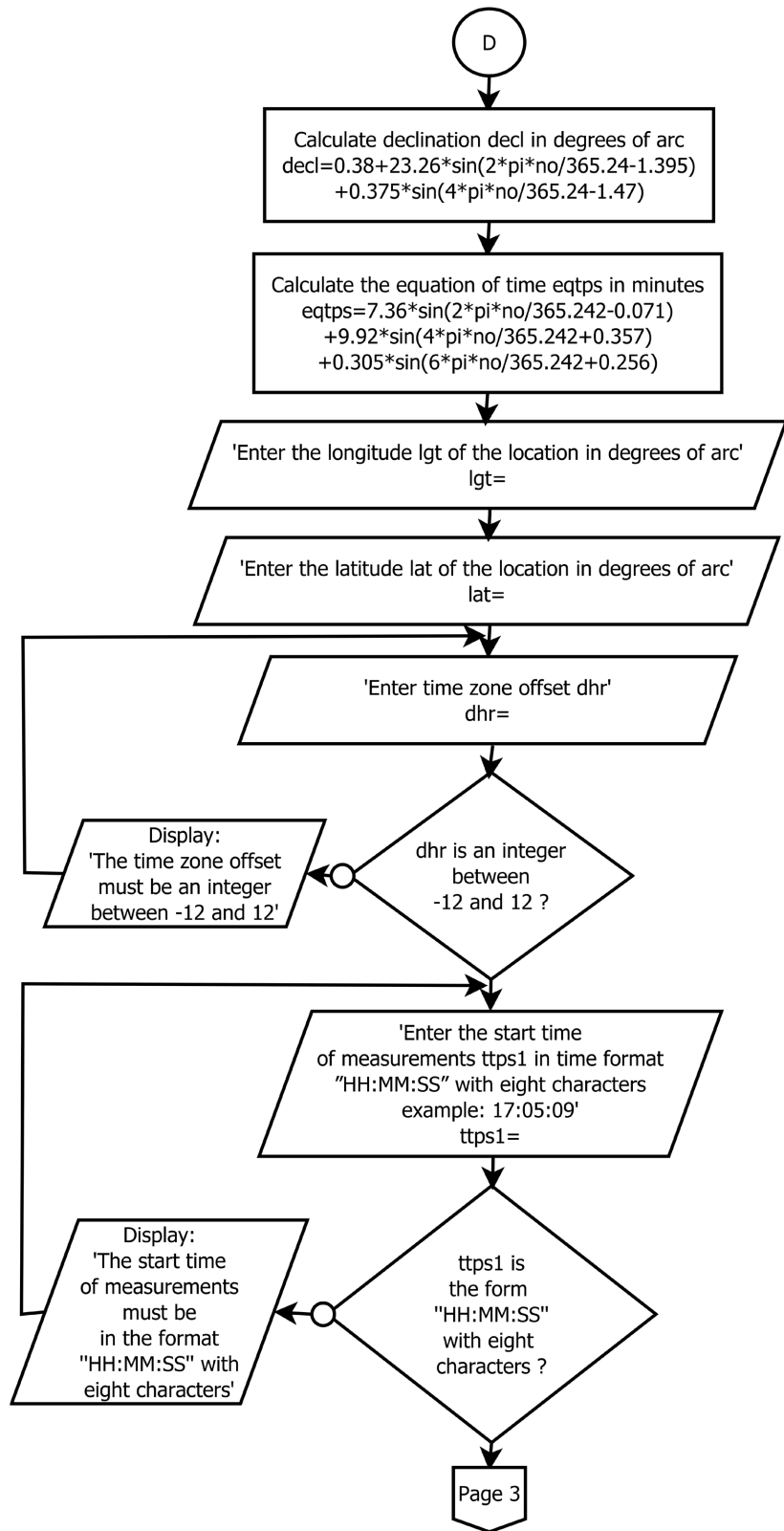


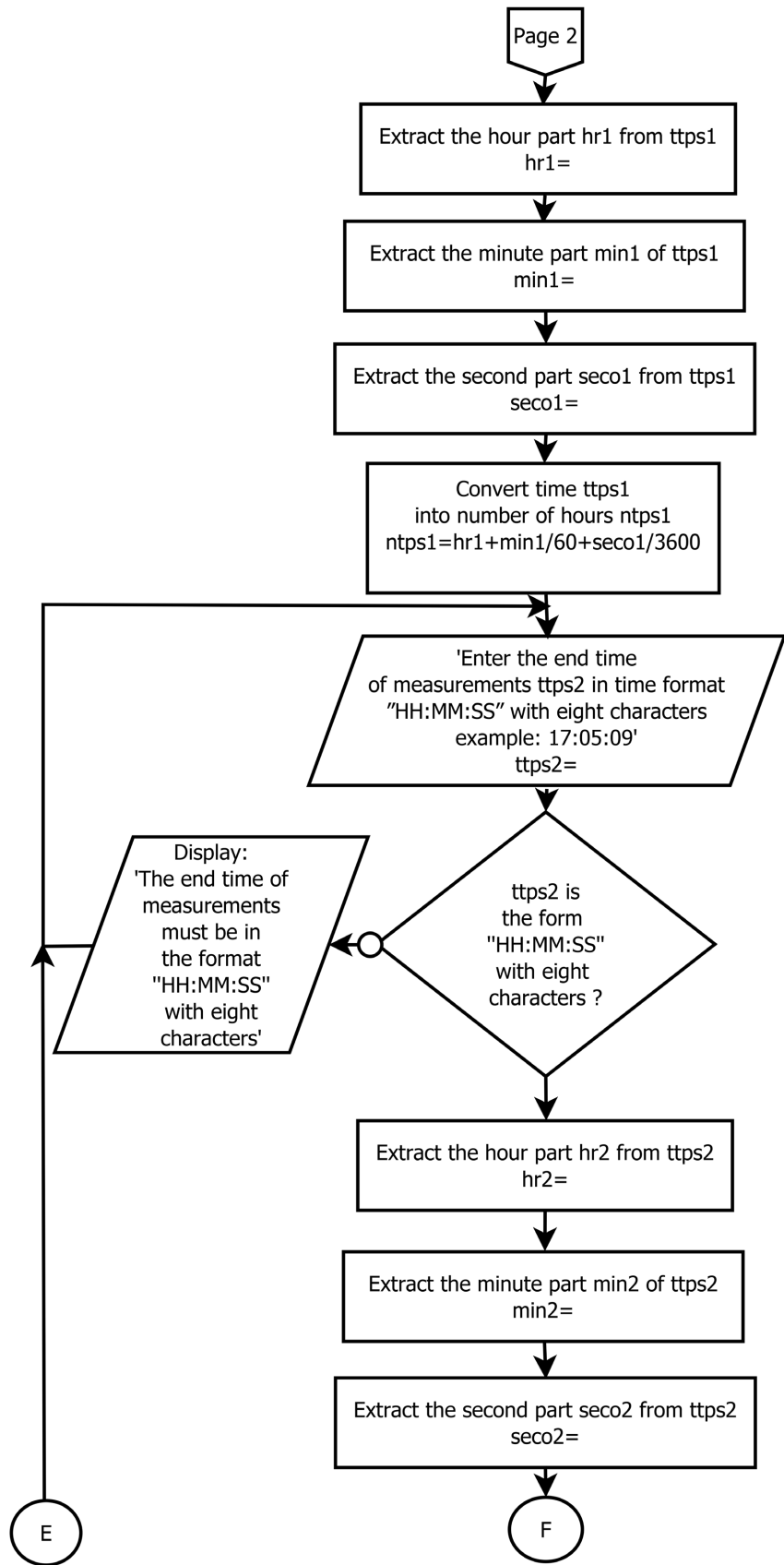
Figure 14. Organization chart on page 1. (a) Organization chart at the top of page 1; (b) Organization chart continued from page 1.





(b)

**Figure 15.** Organization chart on page 2. (a) Organization chart at the top of page 2; (b) Organization chart continued from page 2.



(a)

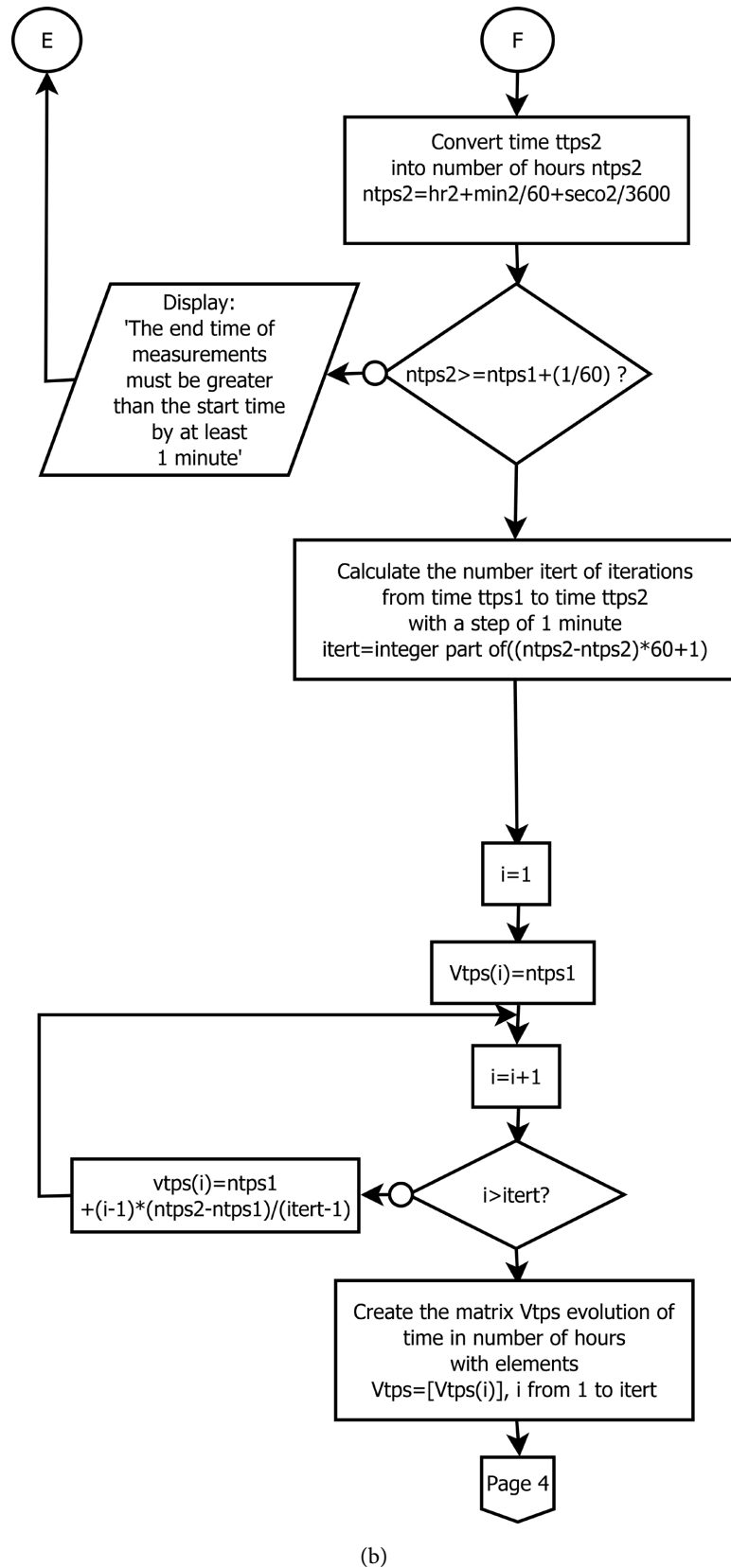


**Figure 16.** Organization chart on page 3. (a) Organization chart at the top of page 3; (b) Organization chart continued from page 3.

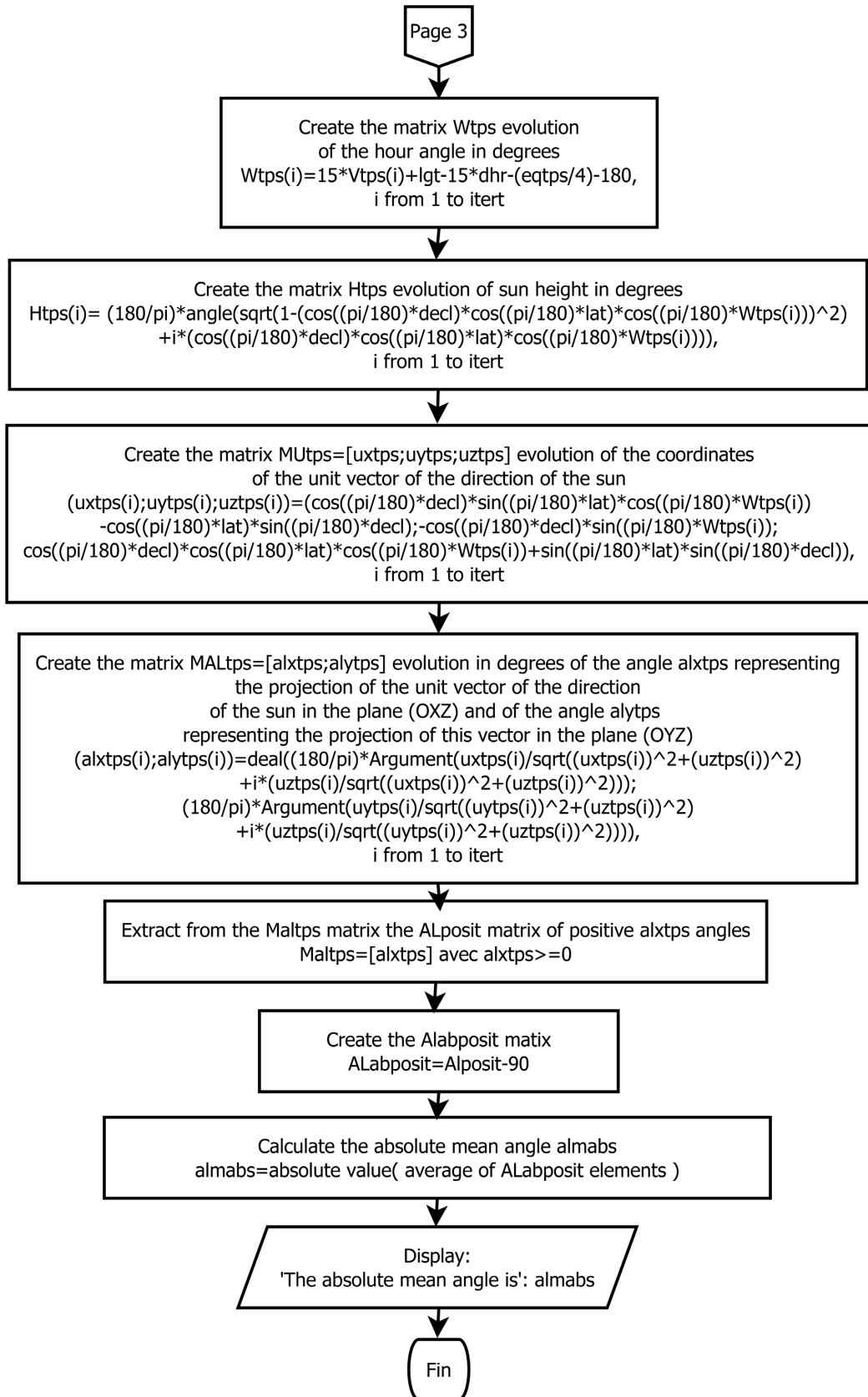


Figure 17. Organization chart on page 4.

### 3. Results and Discussion

It should be noted that, for this series of measurements, the solar distiller is positioned so that its axis 3 ↔ 4 follows the East-West axis.

The central absorber compartment is equipped with a reflector, deflecting solar rays above the distiller towards the entrance of this compartment, in order to increase the direct solar radiation it receives.

In the morning, the surface of the reflector faces east (against the sun), and in the afternoon it faces west.

The plywood covers of compartments 1 and 2 are removed.

In these experiments, we used 3375 l of tap water for each tank, corresponding to a height of solution to be distilled in each tank equal to 1 cm.

**Table 1** shows eleven days of measurements with their daily irradiations, absolute mean angles  $\overline{\alpha_{ax}}$  and corresponding productivities.

**Table 1.** Irradiation, absolute mean angle, productivity of the distiller.

Day	Daily irradiation in kWh/m <sup>2</sup>	Absolute mean angle $\overline{\alpha_{ax}}$ in degrees of arc (°)	Productivity in kg/m <sup>2</sup>
01/03/2017	3.9208	19.7906	2.9728
15/03/2017	4.9134	10.3490	4.0552
25/03/2017	4.5420	2.7534	3.8955
26/03/2017	5.0390	2.5586	4.4725
29/03/2017	5.3035	2.8040	4.8205
01/04/2017	4.7479	4.5603	3.9215
05/04/2017	4.8251	7.4826	4.0072
08/04/2017	4.4324	9.4444	3.6548
11/04/2017	4.9743	11.0925	4.2125
12/04/2017	3.8678	11.6768	3.0789
16/02/2018	4.2384	25.8356	2.9972
<b>Standart deviations</b>	0.4425	7.0479	0.5767

#### 3.1. Correlations: Daily Irradiation and Productivity

The Student's t.test for a two-tailed distribution of samples measuring daily irradiation matched to samples measuring productivity of size 11, gives a p-value equal to

$$1.2539 \times 10^{-7} < 0.01.$$

This Student's t.test shows that there is a highly significant correlation between productivity and daily irradiation.

The coefficient of determination of productivity as a function of daily irradiation is  $R^2 = 0.9289$ , close to 1.

This sends to study the linear correlation between productivity and daily

irradiation. **Table 1** was used to construct **Figure 18**, showing the scatterplot of productivity as a function of daily irradiation.

In **Figure 18**, the arrangement of the scatterplot of productivity as a function of irradiation allows a linear fit with the regression line:

$$y = 1.2599 \times x - 1.9743 \quad (15)$$

This correlation is strong because the correlation coefficient  $r = 0.9638$  is close to 1.

Productivity therefore depends on daily irradiation and increases with daily irradiation.

This is because solar irradiation is the main source of energy used to heat and vaporise the water needed for distillation.

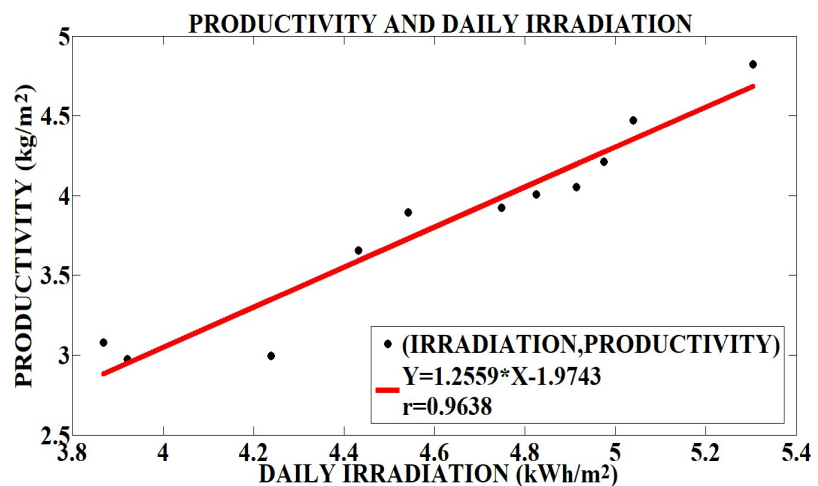


**Figure 18.** Linear correlations between irradiation and productivity.

### 3.2. Correlations: Absolute Mean Angle and Productivity

The Student's t.test for a two-tailed distribution of samples measuring the absolute mean angle matched to samples measuring productivity of size 11, gives the p-value equal to

$$0.0296 < 0.05.$$

This Student's t.test shows that there is a significant correlation between productivity and absolute mean angle.

The coefficient of determination for productivity as a function of absolute mean angle is

$$R^2 = 0.6333, \text{ greater than } 0.5.$$

Let's look at the linear correlation between absolute mean angle and productivity.

**Table 1** was used to construct **Figure 19**.

In **Figure 19**, the arrangement of the scatter plot of productivity as a function of the absolute mean angle  $\overline{\alpha_{ax}}$ , allows a linear fit with the regression line:

$$y = -0.0651 \times x + 4.4676 \quad (16)$$

The correlation coefficient is  $r = -0.7958$ .

Productivity therefore depends on the absolute mean angle; when this angle decreases, productivity increases.

The productivity of the distiller depend on the absolute mean angle  $\overline{\alpha_{ax}}$ , that's to say the proximity of the sun's path to the vertical plane passing through the East-West axis.

If we look at **Figure 20** we can see that, because of the "masking effects" due to the geometry of the central compartment and compartments 1 and 2, the closer the sun's path is to the vertical plane passing through the East-West axis (the absolute mean angle  $\overline{\alpha_{ax}}$  is small), the larger the surfaces (on the central absorber and the tanks) directly illuminated by the sun's rays and the closer the solar rays are to the normal to these surfaces, so the conversion of this incident solar radiation into heat is more efficient, resulting in an increase in productivity.

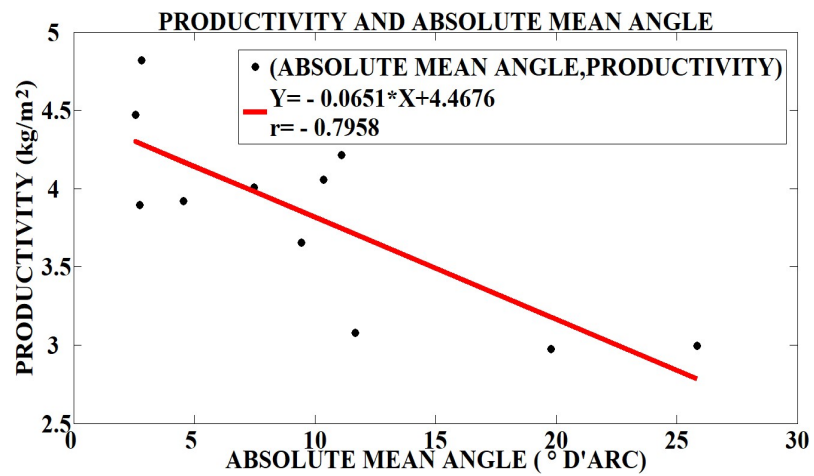


**Figure 19.** Linear correlation between absolute mean angle and productivity.

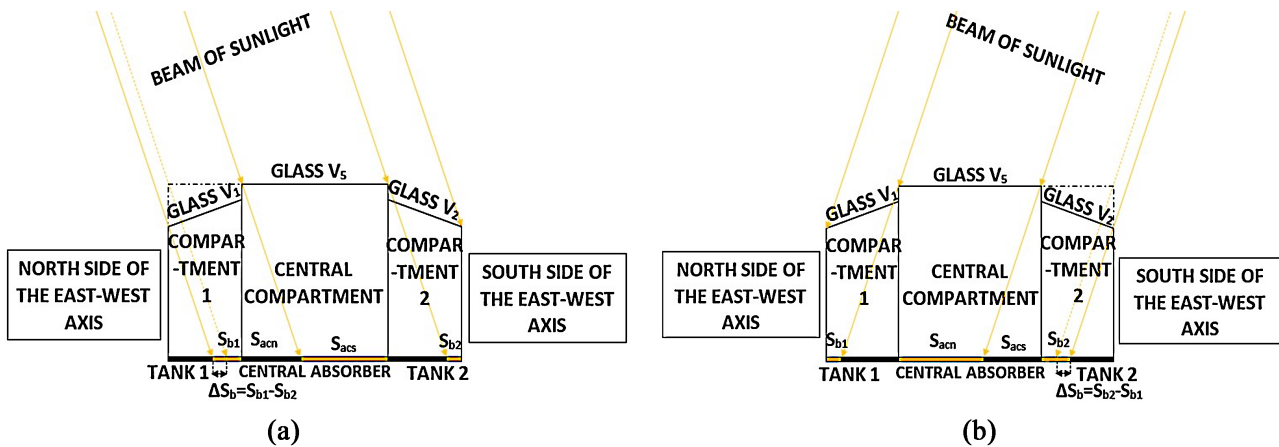


**Figure 20.** Directly illuminated surfaces on the troughs and central absorber according to the sun's position in relation to the East-West axis. (a) Sun is on the North side of the East-West axis; (b) Sun is on the South side of the East-West axis.

If we follow the same reasoning, we understand that moving the sun's path away from the vertical plane passing through the East-West axis (the absolute mean

angle  $\overline{\alpha_{ax}}$  is large) will cause the decrease in productivity.

### 3.3. Forecast on the Productivity

We have seen that the productivity of the distiller depend on both the daily irradiation and the absolute mean angle  $\overline{\alpha_{ax}}$  over the duration of the measurements.

This explains, on the bar graphs in **Figure 21**, showing productivity as a function of daily irradiation, the decrease in productivity on 1 March 2017 and 16 February 2018, compared with the 12 April 2017 (**Table 1**), despite the fact that the irradiation levels on irradiations on 1 March 2017 and 16 February 2018 were higher than those on 12 April 2017. In fact, in **Table 1**, the absolute mean angles for 1 March 2017 and 16 February 2018 are higher than that of 12 April 2017.

The coefficient of multiple determination of productivity as a function of daily irradiation and absolute mean angle is  $R^2 = 0.979404577$  is close to 1.

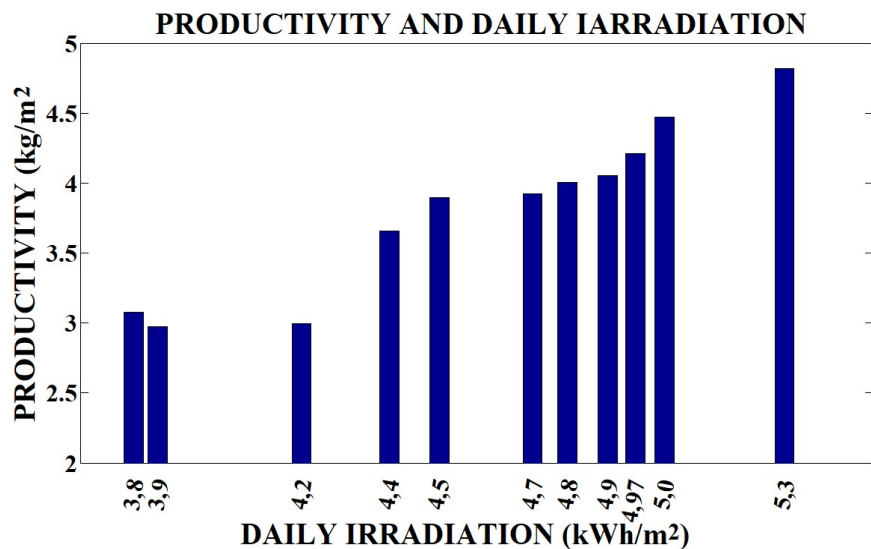


**Figure 21.** Bar graphs of productivity as a function of daily irradiation.

This justifies the use of multiple linear correlation formulas linking productivity to daily irradiation and absolute mean angle, to predict or estimate distiller productivity [4] [5].

Let's call  $X_1$ ,  $X_2$  and  $Y$  the respective physical quantities: daily irradiation over the duration of the measurements in kWh/m<sup>2</sup>, the absolute mean angle  $\overline{\alpha_{ax}}$  in degrees of arc over the duration of the measurements (with  $\alpha_x \geq 0$ ) and productivity in kg/m<sup>2</sup>;

$r_{X_1Y}$ ,  $r_{X_2Y}$  and  $r_{X_1X_2}$  the correlation coefficients between the respective quantities  $Y$  and  $X_1$ ,  $Y$  and  $X_2$ ,  $X_1$  and  $X_2$ ,  $\sigma_{X_1}$ ,  $\sigma_{X_2}$  and  $\sigma_Y$  the standard deviations of the respective quantities  $X_1$ ,  $X_2$  and  $Y$ .

The multiple correlation coefficient  $R_{Y,X_1X_2}$  of productivity as a function of daily irradiation and the absolute mean angle  $\overline{\alpha_{ax}}$ , is given by the formula:

$$R_{Y, X_1 X_2} = \sqrt{\frac{(r_{X_1 Y})^2 + (r_{X_2 Y})^2 - 2 \times (r_{X_1 Y}) \times (r_{X_2 Y}) \times (r_{X_1 X_2})^2}{1 - (r_{X_1 X_2})^2}} \quad (17)$$

The linear equation that gives productivity as a function of irradiation and the absolute mean angle  $\overline{\alpha_{ax}}$  is:

$$Y = A_{X_1 Y, X_2} \times X_1 + A_{X_2 Y, X_1} \times X_2 + B_{Y, X_1 X_2} \quad (18)$$

The partial correlation coefficient  $A_{X_1 Y, X_2}$  of  $Y$  in  $X_1$  when  $X_2$  is constant is such that:

$$A_{X_1 Y, X_2} = \frac{\sigma_Y}{\sigma_{X_1}} \times \frac{r_{X_1 Y} - r_{X_2 Y} \times r_{X_1 X_2}}{1 - (r_{X_1 X_2})^2} \quad (19)$$

The partial correlation coefficient  $A_{X_2 Y, X_1}$  of  $Y$  in  $X_2$  when  $X_1$  is constant is such that:

$$A_{X_2 Y, X_1} = \frac{\sigma_Y}{\sigma_{X_2}} \times \frac{r_{X_2 Y} - r_{X_1 Y} \times r_{X_1 X_2}}{1 - (r_{X_1 X_2})^2} \quad (20)$$

Calculations using the values in **Table 1** give:

$$R_{Y, X_1 X_2} = 0.989648714 \quad (21)$$

This means that productivity is strongly linearly correlated with both irradiation and the mean absolute angle. Using the data in **Table 1**, we obtain the equation giving productivity:

$$Y = 1.006697395 \times X_1 - 0.024139062 \times X_2 - 0.585536498 \quad (22)$$

We find the following average errors on productivity:

- $\overline{\Delta Y_1} = \text{average}(|Y_{1mes} - Y_{1cal}|)$ , the mean of the productivity errors calculated using the linear regression formula (15);
- $\overline{\Delta Y_2} = \text{average}(|Y_{2mes} - Y_{2cal}|)$ , the mean of the errors in productivity calculated using the linear regression formula (16);
- $\overline{\Delta Y} = \text{average}(|Y_{mes} - Y_{cal}|)$ , the average error in productivity calculated using the linear regression formula (22).

The indices “mes” and “cal” refer to the measured and calculated values respectively.

The error on the calculation of the productivity with the formula (15) is such that:

$$\left\{ \begin{array}{l} \overline{\Delta Y_1} = 0.127065461 \text{ kg/m}^2 \\ \text{with a frame of error} \\ 0 \text{ kg/m}^2 \leq \overline{\Delta Y_1} \leq 0.351545991 \text{ kg/m}^2 \end{array} \right. \quad (23)$$

The error on the calculation of the productivity with the formula (16) is such that:

$$\left\{ \begin{array}{l} \overline{\Delta Y_2} = 0.304384035 \text{ kg/m}^2 \\ \text{with a frame of error} \\ 0 \text{ kg/m}^2 \leq \overline{\Delta Y_2} \leq 0.628516033 \text{ kg/m}^2 \end{array} \right. \quad (24)$$

The error on the calculation of the productivity with the formula (22) is such that:

$$\begin{cases} \overline{\Delta Y} = 0.070499419 \text{ kg/m}^2 \\ \text{with a frame of error} \\ 0 \text{ kg/m}^2 \leq \overline{\Delta Y} \leq 0.162544132 \text{ kg/m}^2 \end{cases} \quad (25)$$

Relations (23), (24) and (25) have allowed to write:

$$\begin{cases} \overline{\Delta Y} < \overline{\Delta Y}_1 \\ \overline{\Delta Y} < \overline{\Delta Y}_2 \end{cases} \quad (26)$$

From the relation (26), we can say that the multiple correlation formula (22) gives a better approximation than the simple correlation formulas (15) and (16).

#### 4. Conclusions

In view of the results obtained, it can be said that from formula (22) for multiple linear correlations of productivity as a function of both irradiation and the absolute mean angle, we can predict with a good approximation the productivity of the of the five-compartment solar distiller (when its length is positioned along the the East-West axis) as a function of: the daily irradiation; the longitude, the latitude and the time zone offset of the location; the date of the day; the start and end times of the distiller's exposure to the sun.

In view of the small size of the measurement samples, a more detailed study will be carried out with a larger sample size, over different periods and in different locations.

More sophisticated models such as non-linear regression or machine learning algorithms can also be explored, to improve accuracy and prediction potential.

#### Conflicts of Interest

The authors declare no conflicts of interest regarding the publication of this paper.

#### References

- [1] Bechki, D. (2011) Comparative Study and Optimization of Solar Distillation Processes for the Production of Drinking Water in Arid Saharan Zones. Doctoral Thesis, University of Hadj Lakhdar Batna, Batna.
- [2] Chaker, A. and Menguy, G. (2001) International Thermal Days. In: *Internal Efficiency of a Spherical Solar Distiller*. Renewable Energy Review, Renewable Energy Development, Algeria, 53-58.
- [3] Bourdin, V. (2014) Simplified Astronomical Calculations. Master Course PAM 2nd Year, Renewable Energy—Olar Thermal Energy, University of Paris-Sud Orsay.
- [4] Howell, D.C. (2008) Statistical Methods in Human Sciences. Deboeck Superieur.
- [5] Cousineau, D. (2004) Analysis Techniques in Psychologie. Master Course 1st Year, University of Montreal Fall.

## Nomenclature

$\overline{\alpha_{ax}}$	Absolute mean angle (of arc)
$\delta$	Declination (of arc)
$\lambda$	Longitude (of arc)
$a$	Azimuth of the sun (of arc)
$E$	Solar Irradiance in (W/m <sup>2</sup> )
$h$	Height of the sun (of arc)
$k$	Pyranometer coefficient of proportionality ( $k = 10.41 \times 10^{-3} \text{ mV} \cdot \text{m}^2/\text{W}$ )
$L$	Latitude (of arc)
$P_r$	Productivity (kg/m <sup>2</sup> )
$W$	Hour angle (of arc)
U.S.B	Universal Serial Bus for computer science